Solitons in the Peierls condensate. II. Amplitude solitons

Baruch Horovitz
Department of Physics, Ben-Gurion University of the Negev, P. O. Box 653, 84 105 Beer-Sheva, Israel
(Received 31 July 1986)

Charge-density waves whose phase is constrained have amplitude solitons. Exact soliton and soliton lattice solutions for an electron-phonon system in one dimension are constructed by a mapping into the sine-Gordon system. The method is extended to systems with an extrinsic gap parameter as in $(AB)_x$ polymers. Soliton-soliton interactions in the continuum limit are exponential and repulsive. Discrete lattice effects lead to competing interactions which decay as the inverse distance: an attractive force from the finite momentum cutoff and a (usually stronger) repulsive force from coupling with acoustic phonons.

I. INTRODUCTION

The ground state of an interacting one-dimensional electron-phonon system in the adiabatic limit is a charge-density wave (CDW). This result, known as the Peierls theorem,[1,2] has been the basis for an understanding of CDW phenomena in a large variety of compounds in the last decade.[3]

Of particular interest are nonlinear excitations in CDW's, known as solitons. In general, the CDW has a complex order parameter[2] $\Delta\exp(i\phi)$ with Δ its amplitude and ϕ its phase. The ion displacement pattern has the form $\sim\Delta\cos(2k_Fx+\phi)$, where k_F is the electrons' Fermi wave vector; thus, a change in ϕ represents a CDW translation. In a commensurate system of order M the wavelength $\lambda=2\pi/2k_F$ is a rational multiple of the lattice constant a, $\lambda=Ma/N$ ($M>N$ reduced integers). The ground state is then degenerate with ϕ being a multiple of $2\pi/M$.

In Ref. 4 (hereafter denoted as I) the theory of phase solitons was presented. A phase soliton is a localized phase change of $2\pi/M$, such that $\phi(x)$ interpolates between degenerate ground states and Δ is essentially constant. Phase solitons are the charged excitations of commensurate CDW's with $M\geq 3$.

The case $M=2$, i.e., the CDW represents dimerization of the lattice, deserves special attention. The ion distortions at $x=na$ have the form $\Delta\cos(\pi n+\phi)=(-1)^n\Delta\cos\phi$. The degenerate ground states are at $\phi=0,\pi$, i.e., at $\pm\Delta$. Phase solitons are still possible in this system when two types of phonons are coupled with almost equal coupling constants (see I). As ϕ changes from 0 to π, a CDW of the form $(-1)^n\Delta'\sin\phi$ develops and the overall amplitude $[\Delta^2+(\Delta')^2]^{1/2}$ is roughly constant.

The conventional case of a dimerized CDW is concerned with a single phonon and then only the product $\Delta\cos\phi$ is relevant. A pattern in $\phi(x)$ which changes from 0 to π is equivalent to a $\Delta(x)$ connecting the ground states $\pm\Delta_0$. This situation is an amplitude soliton which is studied in the present work. Such solitons were predicted and found in polyacetylene,[5,6] and continuum-model theories yielded exact solutions for $\Delta(x)$.[7,8] The single-soliton solution was in fact known also in the studies of the Gross-Neveu field theory model.[9,10]

In the present work I summarize in Sec. II the derivation of Dashen, Hasslacher, and Neveu[9] (DHN), which is the most systematic derivation of the single-soliton solution. The existence of multisoliton configurations, or a soliton lattice, was first demonstrated in a numerical study[11] of a discrete model. In the continuum-model, exact analytic solutions are available.[12,13] In Sec. III the method for finding soliton lattice solutions is shown in detail. This provides the details of the short presentation in Ref. 12. In Sec. IV modifications of the continuum-model solution due to lattice discreteness effects are discussed. This is of particular importance for finding the long-range soliton-soliton interaction. In the continuum limit this interaction is repulsive and decays exponentially with distance.[14] Lattice discreteness introduces two competing long-range interactions decaying as the inverse distance. One term is attractive and comes from a finite momentum cutoff while the second is repulsive and comes from the coupling with acoustic phonons. Section IV extends the soliton and soliton lattice solutions to the case of $(AB)_x$ polymers[15,16] where a competing gap α limits the range where a dimerized ground state is possible. A soliton lattice, however, is possible even out of this range. The Appendix presents a derivation of the continuum model.

A third part in this series on CDW solitons is Ref. 2, hereafter referred to as III. In III the case of mixed phase-amplitude solutions is considered,[17,18] i.e., both $\phi(x)$ and $\Delta(x)$ have nontrivial variations. The notion of solitons is extended to spin-density wave systems,[19,20] and a general classification of solitons is given in III.

II. THE MODEL AND SINGLE SOLITONS

The continuum model can be derived from a variety of discrete models[21] as shown in the Appendix. The electron field $\psi(x)$ is decomposed into right and left moving fields $u(x)$ and $v(x)$, respectively. The latter represent electron states near the two Fermi points $k_F=\pm\pi/2a$ (a is the lattice constant)

$$\psi_s(x)=u_s(x)\exp(i\pi x/2a)-iv_s(x)\exp(-i\pi x/2a)\ . \qquad (1)$$

The index s has N_s values and represents the number of internal degrees of freedom: $N_s=1$ for spinless fermions describing a spin-Peierls model,[22] $N_s=2$ for electrons with two spin states, and $N_s=4$ for orbital degeneracy.[23]

The fields $u_s(x),v_s(x)$ are considered as slowly varying independent fields. This is justified in weak coupling when only states near the Fermi level are important. The ion displacement pattern is $\sim\Delta(x)\cos(\pi x/a)=(-1)^n\Delta(na)$ for $x=na$. The real field $\Delta(x)$ couples the right and left moving fields and the Hamiltonian is

$$H=\sum_s\int dx\left[iv_F\left[u_s^\dagger(x)\frac{\partial}{\partial x}u_s(x)-v_s^\dagger(x)\frac{\partial}{\partial x}v_s(x)\right]+\Delta(x)[u_s^\dagger(x)v_s(x)+v_s^\dagger(x)u_s(x)]\right]+\int dx\,\Delta^2(x)/(2\lambda\pi v_F)\ . \tag{2}$$

The first term is the electron kinetic energy with a linearized spectrum around the Fermi points with Fermi velocity v_F (as in I). The last term is the lattice elastic energy which resists the distortion $\Delta(x)$; λ is the dimensionless electron-phonon coupling constant (see Appendix).

I consider the adiabatic limit so that $\Delta(x)$ is static and an ion kinetic term $\sim\dot{\Delta}^2$ is absent in (2). Thus, $\Delta(x)$ is a classical field and its equation is obtained by minimizing the expectation value $\langle H\rangle$; $\delta\langle H\rangle/\delta\Delta(x)=0$ yields

$$\Delta(x)=-\lambda\pi v_F\sum_{n,s}{}'[u_n^*(x)v_n(x)+\text{H.c.}]\ . \tag{3}$$

The sum $\sum'$ is on the occupied state labeled by n and s; in most of the following the spin index is not important and is omitted in (3).

The electrons in the potential $\Delta(x)$ have eigenfunctions $u_n(x),v_n(x)$ and eigenvalues ε_n which solve the coupled equations

$$\begin{aligned}\varepsilon_n u_n(x)&=iv_F\frac{\partial}{\partial x}u_n(x)+\Delta(x)v_n(x)\ ,\\ \varepsilon_n v_n(x)&=-iv_F\frac{\partial}{\partial x}v_n(x)+\Delta(x)u_n(x)\ .\end{aligned} \tag{4}$$

For a given $\Delta(x)$ the solutions of (4) must also satisfy Eq. (3), known as the self-consistency equation.

A similar set of equations was studied in I where the method of derivative expansions was developed. If $u_n(x),v_n(x)$ can be solved as a power expansion in derivatives of $\Delta(x)$ and $\phi(x)$, then the electron fields can be eliminated and Eq. (3) becomes a nonlinear equation for $\Delta(x)$ and $\phi(x)$. The derivative expansion, however, involves powers of $\Delta'(x)/\Delta(x)$ and hence fails for an amplitude soliton, for which $\Delta(x)$ passed through zero.

The ground state for a $\frac{1}{2}$-filled band is a constant $\Delta(x)=\Delta_0$ and the Fermi vector then matches the distortion wavelength $2k_F=\pi/a$. The eigenvalues $\pm(v_F^2k^2+\Delta_0^2)^{1/2}$ have a gap $2\Delta_0$ at $k=0$ and the total energy is

$$\langle H\rangle_0=-N_s\sum_k(v_F^2k^2+\Delta_0^2)^{1/2}+\Delta_0^2L/(2\lambda\pi v_F)\ , \tag{5}$$

where L is the length of the system. The ground state Δ_0 is determined by the minimum for $\langle H\rangle_0$:

$$\frac{N_s}{\pi}\int_0^\Lambda dk\frac{1}{(v_F^2k^2+\Delta_0^2)^{1/2}}=\frac{1}{\lambda\pi v_F}\ , \tag{6}$$

where $\Lambda=\pi/2a$ is a momentum cutoff in the electronic spectrum. In weak coupling, $v_F\Lambda\gg\Delta_0$ and[1,2]

$$\Delta_0=2v_F\Lambda\exp(-1/N_s\lambda)\ . \tag{7}$$

Note that in the incommensurate limit the factor in the exponent is $-2/N_s\lambda$.[21] The reason is that the $\pm2k_F$ distortions are then distinct, the elastic energy cost is doubled, and Δ_0 is exponentially smaller.

To find soliton solutions of (3) and (4) most approaches involved guesswork to some degree.[7,8,10,11] The only systematic method is due to DHN and is shown below, including derivation of soliton-soliton interaction and finite cutoff corrections.

The basic idea of DHN is to express $\langle H\rangle$ in terms of scattering data, i.e., reflection coefficient $r(k)$ for a wave vector k and bound states which decay as $\exp(-k_i|x|)$. The variation which leads to Eq. (3) is equivalent to finding extrema of $\langle H\rangle$ with respect to the scattering data. The scattering data, thus determined, then yield the potential $\Delta(x)$ via the inverse scattering technique.

Instead of the two coupled first-order equations (4) it is more convenient to define $f_n(x)=u_n(x)+iv_n(x)$ and obtain a second-order equation

$$\left[-v_F^2\frac{\partial^2}{\partial x^2}+\Delta^2(x)-v_F\Delta'(x)\right]f_n(x)=\varepsilon_n^2f_n(x) \tag{8}$$

decoupled from the equation for $u_n(x)-iv_n(x)$ (see Sec. III). The asymptotic value of the potential $\Delta^2(x)-v_F\Delta'(x)$ is Δ_0^2 so that the bound-state wave vectors k_i with $f_i(x)\to\exp(-k_i|x|)$ satisfy $\varepsilon_i^2=\Delta_0^2-v_F^2k_i^2$. Applying a trace identity (Appendix B of DHN[9]) yields

$$\int_{-\infty}^{\infty}[\Delta^2(x)-\Delta_0^2]dx/v_F^2=-\int_{-\infty}^{\infty}\ln(1-|r(k)|^2)dk-4k_0\ , \tag{9}$$

where a soliton pair (SS) is considered so that $\int\Delta'(x)dx=0$. A single bound state of (8) with index $i=0$ [i.e., two bound states at $\pm\epsilon_0$ of (4)] is considered since keeping the sum over the bound states leads to linearly additive energies and therefore to no new bound states.

Consider the expectation value of Eq. (2) $\langle H\rangle$ relative to $\langle H\rangle_0$ of the ground state:

$$\langle H\rangle-\langle H\rangle_0=N_s\sum_{\varepsilon_n<0}(\varepsilon_n-\varepsilon_n^0)+n_0\varepsilon_0+\int_{-\infty}^{\infty}[\Delta^2(x)-\Delta_0^2]dx/(2\lambda\pi v_F)\ . \tag{10}$$

The first term is the change in electronic energy of all the occupied states, $\varepsilon_n<0$ (including the bound state at $-\varepsilon_0$), while $n_0\le N_s$ is the occupancy of the bound state at energy $+\varepsilon_0$. The three possible occupations for $N_s=2$ are shown in Fig. 1. Using the phase shift $\delta(k)$ the boundary condition $2\pi n=kL+\delta(k)$ implies a shift in $\varepsilon(k)=\pm(v_F^2k^2+\Delta_0^2)^{1/2}$ of the extended states from $\varepsilon_n^0=\varepsilon(2\pi n/L)$ to

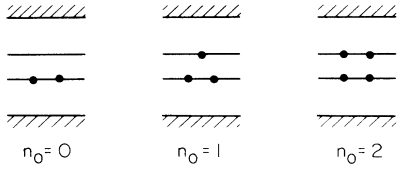

FIG. 1. Energy levels for a two-soliton system with two spin states $N_s=2$. The upper state is occupied by n_0 fermions.

$$\varepsilon_n=\varepsilon\left[\frac{2\pi n}{L}-\frac{\delta(k)}{L}\right]=\varepsilon_n^0-\frac{\partial\varepsilon}{\partial k}\frac{\delta(k)}{L}+O(L^{-2}) . \tag{11}$$

Including the bound state at $-\varepsilon_0$ which was pulled out of the energy $-\Delta_0$, the first term of (10) becomes

$$N_s\sum_{\varepsilon_n<0}(\varepsilon_n-\varepsilon_n^0)=N_s\left[\int_0^\Lambda\frac{\partial\,|\,\varepsilon(k)\,|}{\partial k}\delta(k)dk/\pi-\varepsilon_0+\Delta_0\right] . \tag{12}$$

The scattering data $r(k),k_i$ also determine $\delta(k)$ (Ref. 9) so that (10) has the form

$$\langle H\rangle-\langle H\rangle_0=N_s[I/\pi-\varepsilon_0+\Delta_0]+n_0\varepsilon_0-2k_0v_F/(\lambda\pi)+F(\,|\,r(k)\,|^2) . \tag{13}$$

F is a function of $|\,r(k)\,|^2$ only and is therefore minimized at $r=0$ and $F(0)=0$; the potential is thus reflectionless. The integral I is

$$\begin{aligned}I&=2\int_0^\Lambda\frac{v_F^2k}{(v_F^2k^2+\Delta_0^2)^{1/2}}\tan^{-1}\left[\frac{k_0}{k}\right]dk\\&=2(v_F^2\Lambda^2+\Delta_0^2)^{1/2}\tan^{-1}\left[\frac{k_0}{\Lambda}\right]-\pi\Delta_0\\&\quad+2v_F^2k_0\int_0^\Lambda\frac{dk}{(v_F^2k^2+\Delta_0^2)^{1/2}}\\&\quad+2(\Delta_0^2-v_F^2k_0^2)^{1/2}\tan^{-1}\left[\frac{\Lambda(\Delta_0^2-v_F^2k_0^2)^{1/2}}{k_0(\Delta_0^2+v_F^2\Lambda^2)^{1/2}}\right] .\end{aligned} \tag{14}$$

The logarithmically divergent integral in (14) is precisely cancelled by the term $-2k_0v_F/\lambda\pi$ in (13) since Δ_0 was chosen to satisfy Eq. (6). This is the analog of the renormalization factor Z used by DHN.[9] Defining $v_Fk_0=\Delta_0\sin\theta$, or $\varepsilon_0=\Delta_0\cos\theta$, and expanding (14) to lowest order in $\Delta_0/v_F\Lambda$ yields

$$\langle H\rangle-\langle H\rangle_0=\Delta_0\left[\frac{2}{\pi}N_s(\sin\theta-\theta\cos\theta)+n_0\cos\theta+\frac{N_s}{3\pi}\left[\frac{\Delta_0}{v_F\Lambda}\right]^2\sin^3\theta\right] . \tag{15}$$

For $n_0<N_s$ a single localized $\Delta(x)$ may result.[17,24] Here, however, we are mainly interested in the fully charged situation, $n_0=N_s$. Since $\Delta_0\ll v_F\Lambda$ the minimum of (15) is at $\theta=\pi/2$. The inverse scattering solution [Eq. (3.28) of DHN[9]] shows that this corresponds to an infinitely separated pair of solitons (SS) with shapes $\pm\Delta_s(x)$ where

$$\Delta_s(x)=\Delta_0\tanh(x/\xi_0) \tag{16}$$

and $\xi_0=v_F/\Delta_0$. Expanding near $\theta=\pi/2$ corresponds to a finite SS distance $r=-\xi_0\ln[(\pi/2-\theta)/2]$ with energy

$$E_{SS}=\frac{2}{\pi}\Delta_0N_s\left[1+2e^{-2r/\xi_0}+\frac{1}{6}\left[\frac{\Delta_0}{v_F\Lambda}\right]^2\right] . \tag{17}$$

The single-soliton energy is then $E_S=N_s\Delta_0/\pi$ with small finite cutoff corrections. The SS interaction is exponentially weak and repulsive.

In the next section the energies in (17) will be rederived via the soliton lattice solution; an additional term, however, will appear when the cutoff is finite which is related to the collective nature of the soliton lattice.

III. SOLITON LATTICE

In this section the soliton lattice solution is derived and is shown to describe the lowest-energy configuration for adding a charge density ρ to the $\frac{1}{2}$-filled band. The solution is found by mapping the present fermion problem into linear boson oscillations in some unknown potential; the latter is then found to be related to the sine-Gordon problem.

Define the linear combinations

$$\begin{aligned}f_n(x)&=u_n(x)+iv_n(x) ,\\g_n(x)&=u_n(x)-iv_n(x) ,\end{aligned} \tag{18}$$

which, from (2) satisfy first-order coupled equations,

$$\begin{aligned}\varepsilon_nf_n(x)&=-iv_Fg_n'(x)+i\Delta(x)g_n(x) ,\\\varepsilon_ng_n(x)&=-iv_Ff_n'(x)-i\Delta(x)f_n(x) .\end{aligned} \tag{19}$$

These functions also satisfy second-order decoupled equations [by applying (19) twice]

$$\left[\varepsilon_n^2+v_F^2\frac{\partial^2}{\partial x^2}-\Delta^2(x)+v_F\Delta'(x)\right]f_n(x)=0 , \tag{20a}$$

$$\left[\varepsilon_n^2+v_F^2\frac{\partial^2}{\partial x^2}-\Delta^2(x)-v_F\Delta'(x)\right]g_n(x)=0 . \tag{20b}$$

The self-consistency equation (3) becomes

$$\Delta(x)=\lambda\pi v_F\sum_n{}'\,\mathrm{Im}[f_n^*(x)g_n(x)] . \tag{21}$$

An $\varepsilon=0$ state does not contribute to Eq. (21) since from Eq. (19) with $\varepsilon_n=0$ both $f_n(x)$ and $g_n(x)$ can be chosen real. Substituting (19) in (21) yields

$$\Delta(x)=-2\lambda\pi v_F\left[\Delta(x)+\tfrac{1}{2}v_F\frac{\partial}{\partial x}\right]\sum_n{}'\frac{|\,f_n(x)\,|^2}{2\varepsilon_n} , \tag{22}$$

where the sum is on occupied states excluding an $\varepsilon=0$ state.

The equivalent boson problem has a potential $U(\psi)$ with degenerate minima so that a classical soliton solution $\psi_s(x)$ is possible.[25] The boson Hamiltonian is

$$\mathscr{H}=\tfrac{1}{2}\Pi^2(x,t)+\tfrac{1}{2}v_F^2[\psi'(x,t)]^2+U[\psi(x,t)] , \tag{23}$$

where $\Pi(x,t)$ is the conjugate momentum to the field

$\psi(x,t)$. The classical soliton satisfies

$$v_F^2\psi_s''(x)=U'[\psi_s(x)]\ , \tag{24}$$

while small fluctuations $\phi(x,t)$ around the soliton, i.e., $\psi(x,t)=\psi_s(x)+\phi(x,t)$, satisfy

$$\left[\frac{-\partial^2}{\partial t^2}+v_F^2\frac{\partial^2}{\partial x^2}-U''[\psi_s(x)]\right]\phi(x,t)=0\ . \tag{25}$$

The key feature of this structure is the existence of a zero-frequency solution to Eq. (11) which is the soliton translation mode $\psi_s'(x)$. Since Eq. (19) also has an $\varepsilon=0$ solution

$$f_0(x)=f_0(0)\exp\left[-\int_0^x\Delta(x')dx'/v_F\right]\ , \tag{26}$$

we require $f_0(x)\sim\psi_s'(x)$ [for a localized soliton (26) is normalizable by virtue of the soliton topology $\Delta(x)\to\Delta_0\mathrm{sgn}x$ for $x\to\pm\infty$]. By comparing Eqs. (20a) and (25) we identify the boson oscillations $\phi(x,t)$ with the fermion eigenfunctions $f_n(x)$ and

$$U''[\psi_s(x)]=\Delta^2(x)-v_F\Delta'(x)=v_F^2\psi_s'''(x)/\psi_s'(x)\ . \tag{27}$$

Here, $\Delta(x)=-v_Ff_0'(x)/f_0(x)$ and $f_0(x)\sim\psi_s'(x)$ were used. Since $f_0(x)>0$ [Eq. (26)] $\psi_s(x)$ is monotonic and we can use ψ_s as an integration variable in Eq. (27), hence Eq. (24) is obtained. Thus the boson problem (25) indeed relates to a classical soliton equation of the form (24).

The problem is now reduced to the determination of the potential $U(\psi)$. This potential determines via (24) both the single-soliton solution and the soliton lattice. We can therefore use the single-soliton solution, as found in Sec. II to construct the potential $U(\psi)$. From (16) and (27) we find

$$U''[\psi_s(x)]=\Delta_0^2[1-2\,\mathrm{sech}^2(x/\xi_0)]\ . \tag{28}$$

Equations (16) and (26) also yield

$$\psi_s'(x)\sim\exp\left[-\int_0^x\tanh(x/\xi_0)dx/\xi_0\right]$$
$$\sim\mathrm{sech}(x/\xi_0)\ . \tag{29}$$

The following form of solution is chosen for convenience:

$$\psi_s(x)=4\tan^{-1}[\exp(x/\xi_0)]\ . \tag{30}$$

The final step is to eliminate the x dependence in Eq. (28) in favor of a ψ_s dependence via Eq. (30) which results in $U''(\psi_s)=\Delta_0^2\cos\psi_s$. We therefore choose the following potential:

$$U(\psi)=\Delta_1^2(1-\cos\psi)\ , \tag{31}$$

with $\Delta_1=\Delta_0$ in the limit of a single soliton. (As found below, $\Delta_1=\Delta_0$ also with a finite soliton density if $\Lambda\to\infty$.) Thus the celebrated sine-Gordon potential[26] is found.

Equation (31) is expected also from the knowledge of the spectra of Eq. (25). The sine-Gordon potential has a single bound state for one soliton (the translation mode) which broadens into a midband for a soliton lattice, as shown in Fig. 2. As verified below, a gap separates all occupied states from all empty states. Other potentials have additional gaps[13] within the occupied and empty states. The location of such gaps means that they do not lower the electron energies while there is an increase in the elastic energy. Thus other potentials besides (31) which solve Eqs. (3) and (4) can lead to a local minimum of $\langle H\rangle$. The sine-Gordon potential (31) provides the global minimum.

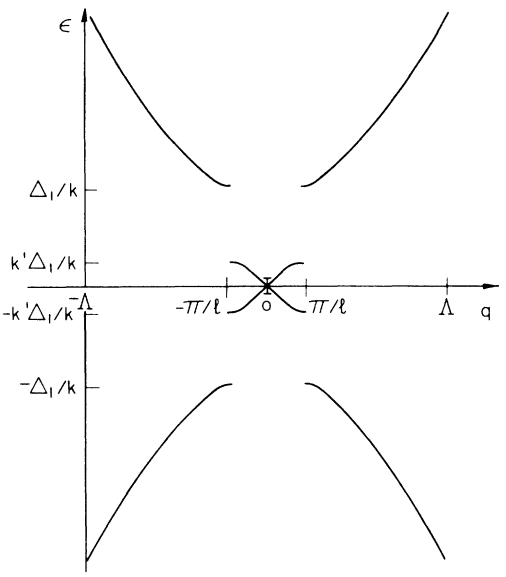

FIG. 2. Energy levels for fermions in a soliton lattice. Note that only two gaps are present at $q=\pm\pi/l$.

I now proceed to present the soliton lattice solution, its fermion eigenfunctions, and check explicitly the self-consistency relation, Eq. (3). The general solution of Eq. (24) with the potential (31) is[25,27,28]

$$\sin\{\tfrac{1}{2}[\psi_s(x)-\pi]\}=\mathrm{sn}(x/k\xi,k)\ , \tag{32}$$

where sn (and cn,dn below) are Jacobian elliptic functions[29] with parameter k, and $\xi=v_F/\Delta_1$. The solution (32) is a lattice of sine-Gordon solitons, with each soliton increasing ψ_s by 2π. The solution (32) satisfies $\psi_s(x+l)=\psi_s(x)\pm2\pi$, where

$$l=2\xi kK(k)\ , \tag{33}$$

where $K(k)$ [and $K'(k),E(k)$ below] being complete elliptic integrals.[29] When $l\gg\xi$ (or $k\to1$), $\psi_s(x)$ is a sequence of well-separated solitons (or antisolitons), each of width ξ and at distance l apart.

The ion displacement pattern $\Delta(x)$ is $\Delta(x)=-v_F\psi_s''(x)/\psi_s'(x)$ [see Eq. (26)], i.e,

$$\Delta(x)=\frac{k\Delta_1\mathrm{sn}(x/k\xi,k)\mathrm{cn}(x/k\xi,k)}{dn(x/k\xi,k)}\ . \tag{34}$$

This pattern (Fig. 3) oscillates between $\pm k\Delta_1/(1+k')$ passing twice through zero in a single period l. [$(k')^2=1-k^2$.]

The eigenvalue equation (20) contains the periodic potential

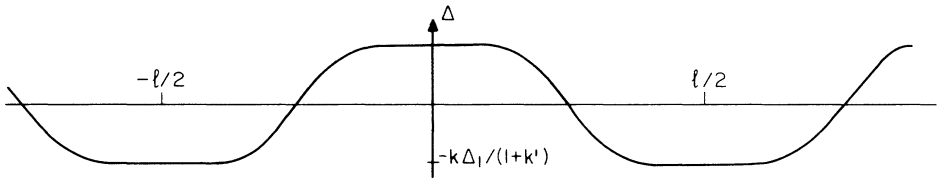

FIG. 3. Schematic structure of the dimerization pattern $\Delta(x)$ for a dilute soliton lattice.

$$\Delta^2(x)-v_F\Delta'(x)=\Delta_1^2\cos\psi_s(x)$$
$$=\Delta_1^2[2\,\mathrm{sn}^2(x/k\xi,k)-1]\ , \tag{35}$$

with period l. The solutions can therefore be labeled by a Bloch wave vector q. Equation (20a) with (35) is Lamé's equation for which the eigenfunctions $f_q(x)$ and eigenvalues ε_q are well known.[27-29] In the boson problem there are two branches: an acoustic branch whose $q=0$ eigenfunction $f_q(x)$ is the translation mode and an optic branch. A single gap at $q=\pm\pi/l$ separates the two branches. In the fermion problem both positive and negative ε_q are allowed. In fact, the pairs $(f_q,-g_q)$ and (f_q,g_q) have eigenvalues $\mp\omega_q$, respectively. Thus the spectrum is symmetric around $\varepsilon=0$ and contains three branches (Fig. 2): the valence band, a midband containing the $\varepsilon=0$ state, and a conduction band.

The midband has eigenvalues $\pm\omega_q$ with

$$\omega_q=(\Delta_1 k'/k)\mathrm{sn}(\chi,k')\ , \tag{36}$$

where χ is determined by q,

$$q=(\Delta_1/v_F k)[E(\chi,k')-\chi(1-E/K)]\ , \tag{37}$$

and $E(\chi,k')$ is the incomplete elliptic integral of the second kind.[29] The range $0<q<\pi/l$ corresponds to $0<\chi<K'$. The eigenfunctions, in terms of the θ_i functions,[29] are

$$f_q(x)=C_q\frac{\theta_3(\pi x/l+i\pi\chi/2k\mid\tau)}{\theta_4(\pi x/l\mid\tau)}e^{iqx}\ , \tag{38}$$

with $\tau=iK'/K$ and C_q is a normalization constant. [The normalization $\int[\,|u_n(x)|^2+|v_n(x)|^2]dx=1$ implies $\int|f_n(x)|^2dx=1$.] After some algebra Eq. (38) yields

$$|f_q(x)|^2=\frac{1}{L}\frac{\mathrm{dn}^2(\chi,k')-k^2\mathrm{sn}^2(x/k\xi,k)}{\mathrm{dn}^2(\chi,k')-1+E/K}\ . \tag{39}$$

In particular, at $\varepsilon=0$, $f_0(x)\sim\psi_s'(x)$,

$$f_0(x)=L^{-1/2}(K/E)^{1/2}\mathrm{dn}(x/k\xi,k)\ . \tag{40}$$

The valence and conduction bands have eigenvalues $\pm\omega_q$, where

$$\omega_q=\frac{\Delta_1}{k}\frac{\mathrm{dn}(\chi,k')}{\mathrm{cn}(\chi,k')}\ , \tag{41}$$

$$q-\pi/l=\frac{\Delta_1}{k}\left[\chi(1-E/K)-E(\chi,k')+\frac{\mathrm{dn}(\chi,k')\mathrm{sn}(\chi,k')}{\mathrm{cn}(\chi,k')}\right]\ . \tag{42}$$

The range of q is $\pi/l<q<\Lambda$, which corresponds to $0<\chi<K'(k)-\epsilon$ with $\epsilon\to0$ as $\Lambda\to\infty$. More precisely, expansion of (42) near $\chi=K'$ yields

$$\Lambda=\frac{\Delta_1}{\epsilon k}\left[1+\epsilon^2\left(\frac{E}{K}-\frac{1+(k')^2}{3}\right)-\epsilon^4\frac{1-(k')^2+(k')^4}{45}+O(\epsilon^6)\right]\ . \tag{43}$$

The eigenfunctions are

$$f_q(x)=C_q'\frac{\theta_4(\pi x/l-i\pi(\chi-K')/2K\mid\tau)}{\theta_4(\pi x/l\mid\tau)}\ . \tag{44}$$

Evaluation of the normalization constant C_q' and some algebra yield

$$|f_q(x)|^2=\frac{1}{L}\frac{\mathrm{dn}^2(\chi,k')-\mathrm{dn}^2(x/k\xi,k)\mathrm{cn}^2(\chi,k')}{\mathrm{dn}^2(\chi,k')-(E/K)\mathrm{cn}^2(\chi,k')}\ . \tag{45}$$

Equations (36) and (41) imply a gap in the spectrum at $q=\pm\pi/l$ at energies $k'\Delta_1/k<|\epsilon|<\Delta_i/k$. It is remarkable that there are no additional gaps at multiples of π/l; this is a manifestation of the reflectionless property of the potential (31).[28] The presence of additional gaps, as mentioned above, increases the total energy and does not yield a global minimum. The numerical solution[11] did show some spurious gaps at multiples of π/l. The reason is that $\Delta(x)$ was represented in this study by a harmonic expansion up to the fifth order. This expansion becomes worse as $l/\xi\to\infty$, in the dilute soliton lattice limit.

The next step is to check the self-consistency relation (22); this will prove the local stability of the solution and will eventually determine Δ_1. We consider a fully charged soliton lattice, i.e., the midband is either empty or fully occupied. The excess fermion density ρ relative to the commensurate situation comes from the states $-\pi/l<q<\pi/l$ with $\varepsilon>0$ ($\varepsilon<0$) when the midband is full (empty). Thus, $\rho=\pm N_s/l$. Since there are two solitons per period the soliton density is $\rho_s=2/l$ and the average charge per soliton is $\pm N_s/2$, as expected from Sec. II.

The midband thus does not contribute to Eq. (22), while the valence band, after changing the integration variable from q to χ yields

$$\frac{1}{N_s\lambda}=\ln\left[\frac{1+\mathrm{sn}(K'-\varepsilon,k')}{\mathrm{cn}(K'-\varepsilon,k')}\right]\ . \tag{46}$$

Note that a factor $\Delta(x)$ cancelled and self-consistency is proven. Expansion of (46) and use of (43) yield

$$\frac{1}{N_s\lambda}=\ln\left[\frac{2\Lambda}{\Delta_1}\right]-\frac{\eta^2}{k^2}\left[\frac{E}{K}-\frac{1+(k')^2}{4}\right]+O(\eta^4)\ , \tag{47}$$

where the expansion parameter is now $\eta=2\exp(-1/N_s\lambda)$ and $\eta=k\varepsilon$ to leading order. The gap Δ_0 in the commensurate situation is from Eq. (6)

$$\Delta_0=2v_F\Lambda e^{-1/N_s\lambda}[1+\eta^2/4+o(\eta^4)]\ , \tag{48}$$

which yields for Δ_1

$$\Delta_1=\Delta_0\left[1-\frac{\eta^2}{k^2}\left[\frac{E}{K}-\tfrac{1}{2}(k')^2\right]+o(\eta^4)\right]\ . \tag{49}$$

In the weak-coupling limit, i.e., $\lambda\to 0$ with $\Lambda\to\infty$ such that Δ_0 is finite, $\eta\to 0$ and $\Delta_1=\Delta_0$.

Finally, I evaluate the energy of the soliton lattice (per unit length) $E_{\rm SL}=\sum_{i=1}^{5}J_i$ with the following five terms:

$$LE_{\rm SL}=\sum_{\rm mid}{}'\varepsilon_n+\sum_{\rm val}{}'\varepsilon_n-\sum{}'\varepsilon_n^0+\frac{\Delta_1^2}{2\lambda\pi v_F}\int[\Delta^2(x)-\Delta_1^2]dx+\frac{\Delta_1^2-\Delta_0^2}{2\lambda\pi v_F}\ . \tag{50}$$

Since the midband is symmetrically occupied, the first term is $J_1=0$. The second term is the sum over the valence band, which after using (46) becomes

$$J_2=-\frac{\Delta_1^2}{\pi\lambda k^2}\left[\frac{1+(k')^2}{2}-\frac{E}{K}\right]-\frac{N_s\Delta_1^2}{\pi}\frac{\mathrm{sn}(K'-\varepsilon,k')}{\mathrm{cn}^2(K'-\varepsilon,k')}\ . \tag{51}$$

The third term is the subtracted energies of the commensurate case

$$J_3=N_s\int_{-\Lambda}^{\Lambda}(v_F^2q^2+\Delta_0^2)^{1/2}dq/2\pi=(N_s/\pi)\Lambda^2[1+(\Delta_0/\Lambda)^2]^{1/2}+\Delta_0^2/(2\pi\lambda v_F)\ . \tag{52}$$

The terms J_4+J_5 are the elastic energy relative to the commensurate situation. Using (34) yields [note that imposing a cutoff Λ on the Fourier expansion of $\Delta(x)$ amounts to negligible $\sim\exp(-\Lambda\xi)$ corrections]

$$J_4=\frac{\Delta_1^2}{\lambda\pi v_Fk^2}\left[(k')^2-\frac{E}{K}\right]\ . \tag{53}$$

Combining all terms yields

$$E_{\rm SL}=\frac{N_s}{2\pi}\Lambda^2\left[1+\left[\frac{\Delta_0}{\Lambda}\right]^2\right]^{1/2}-\frac{N_s\Delta_1^2}{2\pi}\frac{\mathrm{sn}(K'-\varepsilon,k')}{\mathrm{cn}^2(K'-\varepsilon,k')}\ . \tag{54}$$

Note that all terms with a $1/\lambda$ factor have cancelled; this corresponds to cancellation of $\sim\ln\Lambda$ terms. Expansion of (54) and use of (43) and (49) yields after some algebra to the energy per soliton,

$$\frac{E_{\rm SL}}{\rho_s}=\frac{N_s\Delta_0}{\pi k}\left[E-\tfrac{1}{2}(k')^2K+\frac{\eta^2}{k^2}\left[\frac{1+(k')^2}{6}E-\frac{E^2}{2K}-\frac{(k')^2K}{12}\right]+o(\eta^4)\right]\ , \tag{55}$$

where $\rho_s=2/l=(\xi kK)^{-1}$ is the soliton density.

The limit of $\rho_s\to 0$ yields the single-soliton energy with the long-range soliton-soliton interaction. In this limit $k'\to 0$ and $\rho_s\xi_0\to(\ln 4/k')^{-1}$ and (55) yields

$$E_{\rm SL}/\rho_s=\frac{N_s\Delta_0}{\pi}\{1+4e^{-2/\rho_s\xi_0}-\tfrac{1}{2}\eta^2\rho_s\xi_0+\tfrac{1}{6}\eta^2+O[(k')^4\ln 4/k',(k')^2\eta^2,\eta^4]\}\ . \tag{56}$$

The $\rho_s\to 0$ limit yields the single-soliton energy

$$E_s=(N_s\Delta_0/\pi)[1+\eta^2/6+o(\eta^4)]\ ,$$

in agreement with Eq. (17). The term $\eta^2/6$ is a self-energy correction due to a finite cutoff. The interaction terms in (56) are of two types. First there is a repulsive term which decays exponentially with $1/\rho_s$. It is a pairwise interaction—it appeared once for two solitons in Eq. (17) while here each soliton has two neighboring solitons and it appears once for every soliton. This account for the preexponential factor being 4 in (56) as compared with 2 in (17). The most remarkable part of (56) is the attractive interaction $-\eta^2\rho_s\xi_0/2$. For $\eta\neq 0$ the long-range interaction is drastically changed—it decays slowly as l^{-1} and is attractive. This term can be traced back to the reduction in the gap Δ_1 when $\eta\neq 0$. From (49) and a $k'\to 0$ expansion, $\Delta_1\to\Delta_0(1-\rho_s\xi_0\eta^2)$; the presence of the midband [which does not contribute to (22)] reduces the phase space of electron states (of order Λ) by $2\pi/l=\pi\rho_s$. Thus Δ_1 is reduced and the "single-soliton" energy $E_s\sim\Delta_1$ (in the *presence* of a finite soliton density) is also reduced.

Note that the attractive term is absent in Eq. (17). Thus it is not a two-body interaction but a collective effect. This is also clear from the previous phase-space argument. It is the presence of infinite solitons (finite density ρ_s) which lowers the energy per soliton.

A few other properties of the solution are worth noting. The gap E_g in the fermion spectrum is between the top of the midband $\varepsilon_m=k'\Delta_1/k$ and the bottom of the conduction band $\varepsilon_c=\Delta_1/k$ (assuming a filled midband). Thus,

$$E_g=\Delta_1(1-k')/k\ . \tag{57}$$

In the limit of $\rho_s\to 0$, $k'\to 0$, Eq. (57) yields $E_g\to\Delta_0$ which is the midgap distance to the conduction band for a single soliton. The limit of a dense lattice corresponds to $2\pi/l\sim\Lambda$, i.e., the intersoliton distance l becomes of the order of the underlying lattice constant $2\pi/\Lambda$. In this limit $k\to 0$ and $l=2kK\xi\to\pi k\xi$, $k\sim 2/\Lambda\xi$. From (57),

$$E_g\to\Delta_1^2/v_F\Lambda=4v_F\Lambda e^{-2/N_s\lambda}\ \text{ as } l\sim 1/\Lambda\ . \tag{58}$$

This is the Peierls gap for an incommensurate CDW, with $\Delta(x)$ becoming a single sine wave. Note the factor 2 in the exponent of (58). In weak coupling the incommensurate gap is exponentially smaller than the commensurate one.

The chemical potential for fermions is

$$\mu=\frac{2}{N_s}\frac{\partial E_{\rm SL}}{\partial \rho_s}=\frac{2\Delta_0}{\pi k}E\ , \tag{59}$$

since each soliton corresponds to an excess of $N_s/2$ fermions. ($\eta\to 0$ was taken here.) The result (59) satisfies $\varepsilon_m<\mu<\varepsilon_c$; this proves that addition or subtraction of fermions is by rearranging the lattice such that the midgap is precisely full and not by adding a fermion to the conduction band or a hole to the midband.

Consider finally the local fermion density which in terms of the original fields is $\sum_n |\Psi_n(x)|^2$ [see Eq. (1)]. This involves a slowly varying term

$$\rho(x)=\sum_n{}'[\,|u_n(x)|^2+|v_n(x)|^2] \tag{60}$$

and a rapidly varying density

$$\rho_{\rm CDW}(x)=i\exp(i\pi x/a)\sum_n{}' u_n(x)v_n^*(x)+{\rm H.c.} \tag{61}$$

The completeness relation of $[u_n(x),v_n(x)]$ implies that the sum (60) if taken on all states is x independent. In fact, $\frac{1}{2}$ of this sum can be subtracted from (60) as the background charge; by $\pm\varepsilon$ symmetry this subtraction is the sum on valences states plus $\frac{1}{2}$ of the midband states. Hence,

$$\rho(x)=\tfrac{1}{2}\sum_{\rm mid}[\,|u_n(x)|^2+|v_n(x)|^2]\ ,$$

which after some algebra becomes

$$\rho(x)=\frac{N_s}{\pi}\rho_s K\left[E'-\tfrac{1}{2}k^2K'{\rm sn}^2(x/k\xi,k)-\tfrac{1}{2}K'+\frac{(k')^2K'}{2{\rm dn}^2(x/k\xi,k)}\right]\ . \tag{62}$$

The rapidly varying density becomes [using (3)]

$$\rho_{\rm CDW}(x)=\frac{N_s\Delta(x)}{2\lambda\pi v_F}\sin(\pi x/a)+\frac{kK'\Delta'(x)}{\pi\Delta_1}\cos(\pi x/a)\ . \tag{63}$$

IV. COUPLING TO ACOUSTIC PHONONS

In the preceding section it was found that the continuum Hamiltonian (2) led to a remarkable form of soliton-soliton interaction if the momentum cutoff Λ was kept finite. The Hamiltonian (2), however, is derived from a discrete model by neglecting $1/\Lambda^2$ corrections. A consistent procedure is therefore to evaluate also the corrections to the Hamiltonian itself.

I consider here the finite Λ correction of the tight-binding Su-Schrieffer-Heeger (SSH) model.[5] As shown by Maki[30] and in the Appendix, a finite Λ amounts to a coupling between the fermions and the acoustic degrees of freedom.

The ion displacement at site m is written as $u_m=y_m-(-1)^n\Delta_m/4\alpha$, where the acoustic deformation y_m and the dimerization Δ_m are slowly varying fields ($\alpha\sim\sqrt{\lambda}$ is the electron-phonon coupling). Using $x=ma$ with a the lattice constant, the Hamiltonian terms which involve $y(x)$ are

$$H_{\rm ac}=\int dx\{-i\alpha a^2y'(x)[\hat{J}(x)-P]+\tfrac{1}{2}Ka[y'(x)]^2\}\ , \tag{64}$$

where the prime is a space derivative and the operator $\hat{J}$ is

$$\hat{J}(x)=u^\dagger(x)u'(x)-v^\dagger(x)v'(x)+{\rm H.c.} \tag{65}$$

P is an external pressure term which is chosen so that the commensurate system has the prescribed lattice constant a and $\int y'(x)dx=0$. Thus, $P=\langle\hat{J}(x)\rangle_0$ with the expectation value in the commensurate state $\Delta(x)=\Delta_0$.

Equation (22) and its derivative can be used to yield the expectation value

$$J(x)=\langle\hat{J}(x)\rangle=(i/\lambda\pi)[v_F\Delta'(x)-2\Delta^2(x)]-2iv_F\sum_q{}'\varepsilon_q|f_q(x)|^2\ . \tag{66}$$

Considering only low density $\rho_s\to 0$, the midband is neglected in (66) [$\varepsilon_q\sim\exp(-1/\rho_s\xi)$], while for the valence band

$$|f_q(x)|^2\to\frac{1}{L}\left[1-\frac{\Delta_0^2-\Delta^2(x)+v_F\Delta'(x)}{2\varepsilon_q^2}\right]\Big/\left[1-\frac{\rho_s\xi}{\varepsilon_q^2}\right]\ . \tag{67}$$

Using $\sum'1/|\varepsilon_q|=L/\lambda\pi$ yields

$$J(x)=-(i/\lambda\pi)[\Delta^2(x)+\Delta_0^2]-(2i/L)\sum_q{}'\varepsilon_q/(1-\rho_s\xi/\varepsilon_q^2)\ . \tag{68}$$

To subtract P one can use the definition of the single-soliton energy E_s as the $\rho_s\to 0$ limit of

$$\frac{1}{L}\sum_q{}'\varepsilon_q+\int dx\frac{\Delta^2(x)}{2\lambda\pi L}-\frac{1}{L}\sum_q{}'\varepsilon_q^0-\frac{\Delta_0^2}{2\lambda\pi}\to E_s\rho_s\ . \tag{69}$$

Minimizing $\langle H_{\rm ac}\rangle$ with respect to $y'(x)$ yields the soliton-dependent acoustic deformation

$$y'(x)=(i\alpha a/K)[J(x)-P]=\frac{-\alpha a}{\lambda\pi K}[\Delta_0^2-\Delta^2(x)]+\frac{2\alpha a}{K}E_s\rho_s\ . \tag{70}$$

This deformation has two parts: the larger part (by the factor $1/\lambda$) is localized near the soliton, and the second part, which is x independent. The latter part essentially implies a long-range force between solitons.

The first term of (70) represents a localized lattice contraction [$y'(x)<0$], while the second term is a delocalized expansion. The space average effect is

$$\int dx\,y'(x)/L=\frac{-2\alpha a}{K}\left[\frac{\Delta_0}{\lambda\pi}-E_s\right]\rho_s\ , \tag{71}$$

i.e., for $\lambda \ll 1$ the overall effect is lattice contraction.

Maki's result[30] for $y'(x)$, obtained from the single-soliton solution, differs from (70) in two respects. First, the second term of (70) is absent [perhaps due to neglect of $O(\lambda)$ corrections] and secondly $\Delta_0^2-\Delta^2(x)$ is replaced by $v_F\Delta'(x)$. The latter replacement is correct for a single soliton, but would imply (incorrectly) a vanishing result for a soliton lattice.

The energy at the minimized value of $y'(x)$ is

$$\langle H_{\rm ac}\rangle=\frac{-2\alpha^2a^3}{K}\int dx\left[E_s\rho_s-\frac{\Delta_0^2-\Delta^2(x)}{2\lambda\pi}\right]^2. \quad (72)$$

The $E_s\rho_s$ term is responsible for a $\sim\rho_s^2$ term in the energy which corresponds to a long-range intersoliton interaction. The term $[\Delta_0^2-\Delta^2(x)]^2$ yields a $\sim\rho_s$ term with exponentially weak corrections which are neglected. Hence,

$$\langle H_{\rm ac}\rangle=\rho_sL\left[\frac{2}{\pi}\Delta_0\left[\frac{a}{\xi_0}\right]^2\rho_s\xi_0c-\frac{\Delta_0}{3\pi\lambda}\left[\frac{a}{\xi_0}\right]^2\right], \quad (73)$$

with $c=1-\lambda$. A gain from the acoustic coupling reduces the single-soliton energy [last term in (73)], while the soliton-soliton interaction decays linearly with distance and is repulsive.

Fixed length boundary conditions can be considered by choosing a ρ_s-dependent pressure P in Eq. (64), such that $\int y'(x)dx=0$, i.e., $P=\int dx\,J(x)/L$. The energy of the acoustic coupling has then the form (73) with $c=1/4\lambda$.

Including the attractive effect of Eq. (56) the coefficient c becomes $c=1-\lambda-2/\pi^2$ for fixed pressure or $c=(1/4\lambda)-2/\pi^2$ for fixed length. For $\lambda\ll1$, $c>0$ and the long-range interaction is repulsive. Figure 4 shows results of a numerical study of the SSH model[31] as defined in the Appendix; fixed length boundary conditions were used. The coupling was chosen such that $\Delta_0/t_0=\frac{2}{3}$, which implies $\lambda\simeq0.31$. The data fit a straight line and are inconsistent with an exponential interaction. The data fit $\varepsilon(\rho_s)\equiv E_{\rm SL}/\rho_sLt_0=0.400+0.012\rho_s\xi_0$. The acoustic effect (dashed line) is from (73) with $c=1/4\lambda$, $\epsilon(\rho_s)=0.399+0.038\rho_s\xi$, while including the finite cutoff effect [Eq. (56)] yields $\epsilon(\rho_s)=0.399+0.029\rho_s\xi_0$. In view of some ambiguity in defining λ [via (6) or its lattice version], it seems that the attractive term in (56) improves the result. Also higher-order corrections may effectively change the $\rho_s\xi_0$ coefficient (see Appendix). E_s itself is reduced from $2\Delta_0/\pi=0.424$ to 0.399 in remarkable agreement with the numerical result.

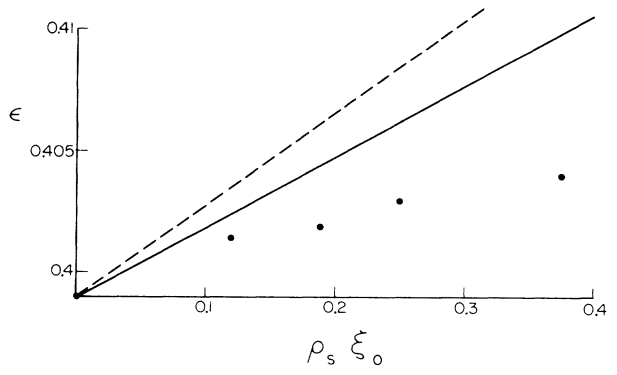

FIG. 4. Energy per soliton from acoustic phonon interaction [Eq. (73)]—dashed line; and including the correction (56)—solid line. The points represent numerical results for a fixed length SSH model (Ref. 31).

In conclusion, the exponential long-range interaction of the continuum limit is radically changed by discreteness, or finite cutoff corrections. The interaction decays as the inverse distance and its sign depends on details of the model; in weak coupling a repulsive interaction is expected.

V. DIATOMIC LATTICE

An interesting modification of the model in Sec. II involves an alternating on-site potential. This potential leads to a gap in the fermion excitation when the band is $\frac{1}{2}$ filled, and therefore competes with the spontaneous gap due to bond dimerization. The on-site potential implies that the unit cell has two sites so that bond dimerization does not change translation symmetry as in Sec. II. Instead, however, the inversion symmetry center at each site is broken and bond dimerization is a proper order parameter.

Experimentally relevant systems are diatomic polymers[15] of the form $(AB)_x$ and organic mixed-stack compounds.[16] In the latter case the interpretation of phase transitions[32] as "neutral-ionic" needs modifications since bond dimerization was indeed found below the transition.[33]

In this section we find the soliton and soliton lattice solutions for the continuum electron-phonon model with alternating on-site potential of strength $\pm\alpha$. The corresponding term in the Hamiltonian is

$$\sum_m(-1)^m\alpha\,|\,\psi(m)\,|^2,$$

where $m=x/a$ is a site index. Using Eq. (1) and neglecting terms which oscillate rapidly with m (as in the Appendix), we find

$$H_D=i\alpha\sum_s\int dx[u_s^\dagger(x)v_s(x)-v_s^\dagger(x)u_s(x)]. \quad (74)$$

The total Hamiltonian is $H+H_D$, where H is given by Eq. (2). The off-diagonal coupling $u_s^\dagger(x)v_s(x)$ has now a complex coefficient $\Delta(x)+i\alpha$. As shown in Fig. 5, the ground states are at $\pm\bar\Delta+i\alpha$ and a soliton would interpolate between these degenerate states. To find $\bar\Delta$, note that the fermion spectrum is $\pm(v_F^2k^2+\bar\Delta^2+\alpha^2)^{1/2}$ so that Δ_0^2 in Eqs. (5)–(7) is replaced by $\bar\Delta^2+\alpha^2$. The energy is then minimized by

$$\bar\Delta=(\Delta_0^2-\alpha^2)^{1/2} \quad (75)$$

if Δ_0 of Eq. (7) satisfies $\Delta_0>\alpha$. If α is too large or the coupling λ too small, i.e., $\alpha>\Delta_0$, the ground state is not bond dimerized ($\bar\Delta=0$).

The unusual soliton charge[15] can be found from (75) even without knowledge of the details of $\Delta(x)$. This is due to the counting rule, proven in I and used extensively in III. The rule shows that the excess charge Q due to a

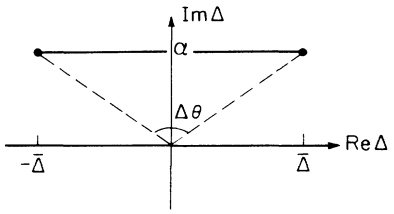

FIG. 5. Ground states and soliton trajectory in the complex plane $\Delta(x)+i\alpha$.

localized configuration is $Q=N_s\Delta\theta/\pi$; $\Delta\theta$ is the phase change of $\Delta(x)+i\alpha$ between the soliton boundaries. As readily seen from Fig. 5,

$$Q=\pm(N_s/\pi)\tan^{-1}(\bar{\Delta}/\alpha)\ , \tag{76}$$

which in general is an irrational value. Spin-carrying solitons have the charge (76) with ± 1 additions.[15,17]

To find explicit solutions I use the transformation (18) to write the fermion eigenvalue equations

$$\begin{aligned}(\varepsilon_n-\alpha)f_n(x)&=-iv_F\frac{\partial}{\partial x}g_n(x)+i\Delta(x)g_n(x)\ ,\\ (\varepsilon_n+\alpha)g_n(x)&=-iv_F\frac{\partial}{\partial x}f_n(x)-i\Delta(x)f_n(x)\ .\end{aligned} \tag{77}$$

The equations can be decoupled by applying a second derivative

$$\left[-v_F^2\frac{\partial^2}{\partial x^2}+\Delta^2(x)-v_F\Delta'(x)\right]f_n(x)=(\varepsilon_n^2-\alpha^2)f_n(x) \tag{78}$$

and a similar equation for $g_n(x)$ with $+\Delta'(x)$. The normalization condition $\int[\,|u_n(x)|^2+|v_n(x)|^2]dx=1$ implies now, by using (77) and (78),

$$\begin{aligned}\int|f_n(x)|^2dx&=(\varepsilon_n+\alpha)/\varepsilon_n\ ,\\ \int|g_n(x)|^2dx&=(\varepsilon_n-\alpha)/\varepsilon_n\ .\end{aligned} \tag{79}$$

A single soliton with, say, $\Delta'(x)>0$ has a level at $\varepsilon=\alpha$ with $g=0$ and

$$f(x)\sim\exp\left[-\int_0^x\Delta(x')dx'\right]\ ;$$

for $\Delta'(x)<0$ a soliton has $\varepsilon=-\alpha$, $f=0$, and

$$g(x)\sim\exp\left[\int_0^x\Delta(x')dx'\right]\ .$$

In general, (79) implies $|\varepsilon_n|\geq\alpha$, i.e., no states can appear in the gap imposed by the α term. To find single-soliton solutions, define a field $\tilde{\Delta}(x)$ by the relation

$$\tilde{\Delta}^2(x)-v_F\tilde{\Delta}'(x)=\Delta^2(x)-v_F\Delta'(x)+\alpha^2\ . \tag{80}$$

Equation (78) has the same form as Eq. (8) with $\Delta(x)$ replaced by $\tilde{\Delta}(x)$. The minimum condition for the total Hamiltonian as a functional of $\tilde{\Delta}(x)$ is identical to that in Sec. II and the energy of a soliton pair is given by Eq. (15). The value of θ which minimizes $\langle H\rangle$ is now constrained by $\varepsilon_0=\Delta_0\cos\theta\geq\alpha$ which relates to the possibility of finding $\Delta(x)$ in terms of $\tilde{\Delta}(x)$ [Eq. (80)]. The polaron solution[34] with $N_s=2$, $n_0=1$ has $\theta=\pi/4$ which is possible only for $\cos(\pi/4)>\alpha/\Delta_0$ or $\alpha<\Delta_0/\sqrt{2}$. For fully charged solitons, $n_0=N_s$, the minimal energy is shifted from $\pi/2$ by the constraint to $\cos\theta=\alpha/\Delta_0$. The two-soliton energy, with total charge N_s, is then

$$2E_s=(4/\pi)[\bar{\Delta}-\alpha\tan^{-1}(\bar{\Delta}/\alpha)]+2\alpha\ . \tag{81}$$

To find the soliton lattice I proceed as in Sec. III and choose the potential (31), i.e.,

$$\Delta^2(x)-v_F\Delta'(x)=\Delta_1^2\cos\psi_s(x)\ , \tag{82}$$

with $\psi_s(x)$ given by (32). The self-consistency equation (21) now becomes

$$\Delta(x)=-2\lambda\pi v_F\left[\Delta(x)+\tfrac{1}{2}v_F\frac{\partial}{\partial x}\right]\sum_n{}'\frac{|f_n(x)|^2}{2(\varepsilon_n+\alpha)} \tag{83}$$

and will eventually determine Δ_1.

The fermion spectrum, shown in Fig. 6, is given by $\varepsilon_q=\pm(\omega_q^2+\alpha^2)^{1/2}$, where ω_q is given by Eqs. (36) and (41). The eigenfunctions are as in Eqs. (38) and (44), except for a normalization change given by Eq. (79). There are now two midbands which are either fully occupied or empty, i.e., the average excess charge is $\pm N_s/l$, with l given by (33). With only the valence band contributing, Eq. (83) becomes

$$\frac{1}{N_s\lambda}=\int_0^{K'-\varepsilon}\frac{\Delta_1\mathrm{dn}^2(\chi,k')d\chi}{k\,\mathrm{cn}^2(\chi,k')\{[\Delta_1\mathrm{dn}(\chi,k')/k\,\mathrm{cn}(\chi,k')]^2+\alpha^2\}^{1/2}} \tag{84}$$

with ε relating to the cutoff Λ via (43). Thus, $\Delta(x)$ of (83) cancels and self-consistency is achieved. When $\alpha=0$, (84) integrates into Eq. (46) with $\Delta_1=\Delta_0$ [terms of order $(\Delta_0/v_F\Lambda)^2$ are neglected in this section]. The $\alpha=0$ equation can be subtracted from (84) to yield a convergent integral as $\varepsilon\to 0$. In terms of the variable $x=\mathrm{sn}(\chi,k')$ this finally yields

$$\ln\left[\frac{\Delta_1}{\Delta_0}\right]=\frac{-\alpha^2k^4}{2\Delta_1^2}\int_0^1\frac{x}{R^3(x)[1-(k')^2x^2]^{1/2}}\ln\frac{1+x}{1-x}dx\ , \tag{85}$$

where

$$R(x)=[1-(k')^2x^2+(k\alpha/\Delta_1)^2(1-x^2)]^{1/2}\ . \tag{86}$$

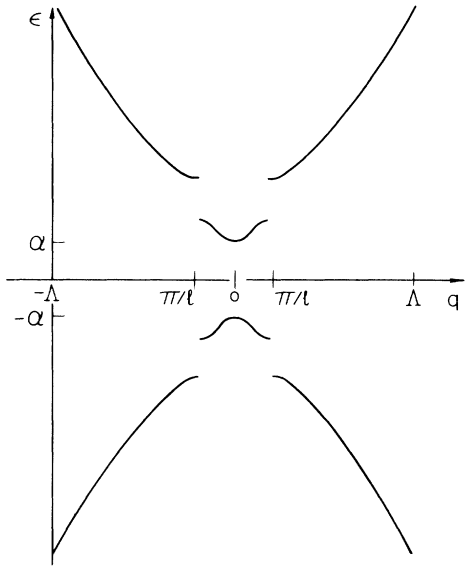

FIG. 6. Energy levels for fermions in a soliton lattice with alternating on-site potential α [Eq. (74)].

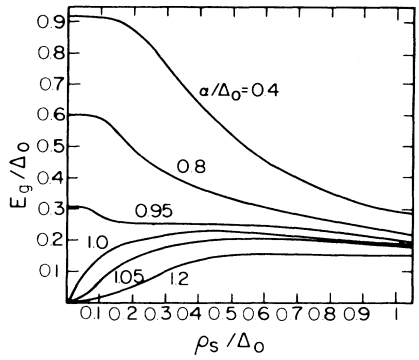

FIG. 7. Gap in the fermion excitation energy for various α [Eq. (74)] as a function of the soliton density.

The gap $E_g=\Delta_1 k/(1+k')$ can be considered as the order parameter of the system. The solutions of Eq. (86) for E_g as a function of $\rho_s=\Delta_1/kKv_F$ are plotted in Fig. 7. For $\alpha<\Delta_0$, $E_g(0)=\bar{\Delta}\neq 0$ and decreases as a function of ρ, except for $0.98<\alpha/\Delta_0<1$, where $E_g(\rho_s)$ has a maximum at a finite ρ_s.

The most interesting situation is found for $\alpha\geq\Delta_0$. In this case the commensurate system is not ordered ($\bar{\Delta}=0$) and the charged excitation are extended electrons or holes. However, as soon as $\rho\neq 0$, a finite order parameter representing localized solitons is generated. It reaches a maximum at a finite ρ (Fig. 7). Thus the addition of charge to a nondimerized system enables the bond ordering to be spontaneously formed.

We can understand this peculiar behavior by considering momentum space where the gap E_g is formed at $q=\pm\pi\rho_s/2$, while the gap 2α remains at $q=0$. Thus for $\rho_s\neq 0$ the competition between the gaps E_g and α is weakened and a finite E_g appears.

The energy of the soliton lattice is obtained with the same steps as in Eqs. (50)—(55). Note that the energy of the $\rho_s=0$ system has a different form when $\alpha<\Delta_0$ ($\bar{\Delta}\neq 0$) or $\alpha>\Delta_0$ ($\bar{\Delta}=0$); this yields different forms for the energy relative to the $\rho=0$ system. After some algebra the soliton-lattice energy $E_{\rm SL}$ becomes

$$\frac{2v_F}{N_s}E_{\rm SL}=\frac{2\Delta_1^2}{\pi k^2}\left[\frac{E}{K}-\tfrac{1}{2}(k')^2\right]+\frac{1}{2\pi}(\Delta_0^2-\alpha^2-\Delta_1^2)+\frac{\alpha^2}{\pi}\ln\left[\frac{\Delta_1}{k\Delta_0}\right]+\frac{\Theta(\alpha-\Delta_0)}{2\pi}\left[\alpha^2-\Delta_0^2-2\alpha^2\ln\left[\frac{\alpha}{\Delta_0}\right]\right]$$
$$+\frac{\Delta_1^2}{\pi k^2}\left[1+(k')^2-\frac{2E}{K}\right]\ln\left[\frac{\Delta_1}{\Delta_0}\right]+\frac{\alpha^2k^2}{\pi}\int_0^1 dx\left[-\left[1+(k')^2-\frac{2E}{K}\right]\frac{x}{2R(x)[1-(k')^2x^2]^{3/2}}\ln\left[\frac{1+x}{1-x}\right]\right.$$
$$\left.+\frac{(1+k^2\alpha^2/\Delta_1^2)[1+(k')^2x^2]-2(k')^2x^4[(k')^2+k^2\alpha^2/\Delta_1^2]}{R^3(x)[1-(k')^2x^2]^2}\times k\ln\left[\frac{k+[1-(k')^2x^2]^{1/2}}{(1-x^2)^{1/2}}\right]\right], \quad (87)$$

where $\Theta(\alpha-\Delta_0)$ is a step function.

To obtain a low-density expansion consider first the $k'\to 0$ limit of (85), which after some algebra yields

$$\Delta_1=\bar{\Delta}\left[1+\left[-\frac{1}{2}+\frac{\Delta_0^2\sin^{-1}(\alpha/\Delta_0)}{\alpha\bar{\Delta}}\right](k')^2+O((k')^4)\right]. \quad (88)$$

This expansion breaks down when $\alpha\to\Delta_0$ or $\bar{\Delta}\to 0$. The energy expansion involves some tedious algebra with the result

$$\frac{2v_F}{\rho_s N_s}E_{\rm SL}=\frac{2\bar{\Delta}}{\pi}+\frac{2\alpha}{\pi}\sin^{-1}\left[\frac{\alpha}{\Delta_0}\right]+\frac{8\bar{\Delta}^2}{\pi\alpha}\sin^{-1}\left[\frac{\alpha}{\Delta_0}\right]\exp\frac{-2\bar{\Delta}}{v_F\rho_s}. \quad (89)$$

The first two terms are the single-soliton energy as given by Eq. (81); more precisely, it is the mean energy of a soliton [$\Delta'(x)>0$] with a fully occupied level at $+\alpha$ and an antisoliton [$\Delta'(x)<0$] with a fully occupied level at $-\alpha$. The last term of (89) is the long-range interaction

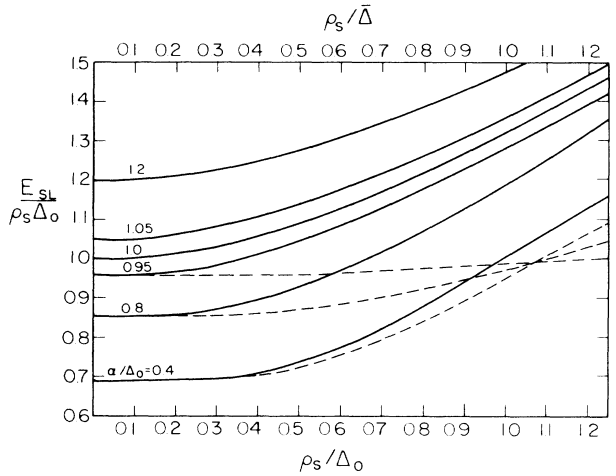

FIG. 8. Energy per soliton for a soliton lattice as a function of $\rho_s v_F/\Delta_0$ (solid curves) and as a function of $\rho_s v_F/\bar{\Delta}$ (dashed curves).

between solitons, which is exponential and repulsive. Since the soliton width is $\sim v_F/\bar{\Delta}$ the factor $-2\bar{\Delta}/v_F\rho_s$ in the exponent measures the overlap between solitons. For a fixed overlap the repulsive interaction becomes weaker as $\alpha\rightarrow\Delta_0$. The energy per soliton is plotted in Fig. 8 as function of ρ_s/Δ_0 and of $\rho_s/\bar{\Delta}$. In the latter case the weaker repulsion as $\alpha\rightarrow\Delta_0$ is apparent. For $\alpha>\Delta_0$ and $\rho_s\rightarrow 0$ the curves approach α, the energy of adding a single fermion or hole to the nondimerized ($\bar{\Delta}=0$) system.

VI. CONCLUSIONS

A method for obtaining an exact soliton lattice solution in continuum theories was shown. The low-density limit of the soliton lattice energy yields beyond a linear term $E_S\rho_s$ the long-range interaction between solitons. In the continuum limit this interaction is exponential and repulsive; finite cutoff or discreteness effects lead to the inverse distance forces, which are repulsive in general. These effects are manifest also in the equivalent sine-Gordon problem, affecting the critical behavior of its commensurate-incommensurate transition.[35]

The soliton lattice solution is an essential tool in deriving properties of near-$\frac{1}{2}$-filled band fermion systems. Thus, optical absorption[36] shows two types of transitions: from the midband with intensity $\sim\rho_s$ for small ρ_s, and valence-to-conduction-band transitions. The sum of both absorption intensities satisfies a sum rule which is independent of ρ_s.

Experimentally, midband transitions were readily observed in polyacetylene, while valence-to-conduction-band transitions were only recently seen by photoinduced absorption.[37] The gap $2\Delta_1/k$ for valence-to-conduction-band transitions (Fig. 2) was found to increase with the doping density [$=2/l$, Eq. (33)], in good agreement with the theory.

The soliton lattice solution was also applied to the spin-density wave system of Cr and its Cr-Mn and Cr-V alloys.[38] In particular, the two-energy-gap structure was obtained by infrared reflectivity.[39]

The spin-Peierls system is an ideal candidate for observing soliton lattices.[12,40] Here a magnetic field acts as a chemical potential for spinless fermions[22] and when it exceeds the single-soliton energy an incommensurate soliton lattice appears. Evidence for such a soliton lattice structure was found by NMR techniques.[41]

In conclusion, details of soliton lattice solutions as presented in this work should provide a basis for comparison with an increasing number of experimental systems. The latter include conducting polymers, such as polyacetylene, $(AB)_x$-type polymers, organic mixed stack compounds, spin-density waves, and spin-Peierls systems.

ACKNOWLEDGMENTS

I thank B. Schaub for his help with the $(AB)_x$ problem. I also thank S. A. Brazovskii, S. Kivelson, and J. R. Schrieffer for stimulating discussions.

APPENDIX

The continuum Hamiltonian with leading corrections is derived here from the tight-binding SSH model[5]

$$H=-\sum_m [t_0-\alpha(R_{m+1}-R_m)](C_n^\dagger C_{n+1}+\text{H.c.}) + \tfrac{1}{2}K\sum_m (R_{m+1}-R_m)^2 . \tag{A1}$$

Here, $C_m, C_m^\dagger$ are electron creation and destruction operators at site m, respectively, R_m is the ion displacement amplitude, t_0 the electron transfer integral, α the electron-phonon coupling constant, and K the elastic constant.

Define now new operators u_m, v_m [Eq. (1) with $x=m/a$]

$$C_m=u_m(i)^m-iv_m(-i)^m . \tag{A2}$$

Decompose also R_m into an acoustic field y_m and a dimerization field Δ_m

$$R_m=y_m-(-1)^m\Delta_m/4\alpha . \tag{A3}$$

All the fields u_m, v_m, y_m, and Δ_m are considered slowly varying and therefore independent fields. Substituting (A2) and (A3) into (A1) and neglecting terms which oscillate rapidly as $\sim(-1)^m$ yields

$$H=-\sum_m [t_0-\alpha(y_{m+1}-y_m)](iu_n^\dagger u_{n+1}-iv_n^\dagger v_{n+1}+\text{H.c.}) - \tfrac{1}{4}\sum_m (\Delta_{m+1}+\Delta_m)(u_n^\dagger v_{n+1}+v_n^\dagger u_{n+1}+\text{H.c.}) + \tfrac{1}{2}K\sum_m (y_{m+1}-y_m)^2+(K/32\alpha^2)\sum_m (\Delta_{m+1}+\Delta_m)^2 . \tag{A4}$$

Expansion to first order, e.g., $y_{m+1}\simeq y(x)+ay'(x)$, yields

$$H = a\int dx[t_0 - \alpha a y'(x)][iu^\dagger(x)u'(x) - iv^\dagger(x)v(x) + \text{H.c.}]$$
$$+ \tfrac{1}{4}\int dx[2\Delta(x) + a\Delta'(x)][u^\dagger(x)v(x) + au^\dagger(x)v'(x) + v^\dagger(x)u(x) + av^\dagger(x)u'(x) + \text{H.c.}] \ . \quad \text{(A5)}$$

Defining $v_F = 2t_0 a$ yields for H the continuum part Eq. (2) plus H_{ac}, Eq. (64). Additional $\sim a^2$ corrections may appear if $u(x), v(x)$ are expanded to second order. These corrections as well as higher-order ones involve diverging k integrals. An efficient method to avoid this[42] is to redefine the transformation (A2) so that the bound spectrum $\cos ka$ appears in the continuum Hamiltonian. The acoustic coupling as well as the ρ_s^2 interaction in Eq. (73) will have then different coefficients, possibly improving agreement with the numerical data in Fig. 4.

[1]R. E. Peierls, *Quantum Theory of Solids* (Clarendon, Oxford, 1955), p. 108.

[2]B. Horovitz, in *Solitons*, edited by S. E. Trullinger, V. E. Zakharov, and V. L. P krovskii (North-Holland, in press).

[3]For recent reviews, see the Proceedings of the International Conference on Synthetic Metals (Kyoto, 1986) [Syn. Met. (to be published)].

[4]B. Horovitz and J. A. Krumhansl, Phys. Rev. B **29**, 2109 (1984).

[5]W. P. Su, J. R. Schrieffer, and A. J. Heeger, Phys. Rev. Lett. **42**, 1698 (1979); Phys. Rev. B **22**, 2099 (1980); **28**, 1138(E) (1983).

[6]For a review, see S. Kivelson, in *Solitons*, edited by S. E. Trullinger, V. E. Zakharov, and V. L. Pokrovskii (North-Holland, in press), and references therein.

[7]S. A. Brazovskii, Pis'ma Zh. Eksp. Teor. Fiz. **28**, 656 (1978) [JETP Lett. **28**, 606 (1978)].

[8]H. Takayama, Y. R. Lin-Liu, and K. Maki, Phys. Rev. B **21**, 2388 (1980).

[9]R. F. Dashen, B. Hasslacher, and A. Neveu, Phys. Rev. D **12**, 2443 (1975).

[10]A. Klein, Phys. Rev. D **14**, 558 (1976); A. Neveu and N. Papanicolao Commun. Math. Phys. **58**, 31 (1978).

[11]A. Kotani, J. Phys. Soc. Jpn. **42**, 416 (1977).

[12]B. Horovitz, Phys. Rev. Lett. **46**, 742 (1981).

[13]S. A. Brazovskii, S. A. Gordyunin, and N. N. Kirova, Pis'ma Zh. Eksp. Teor. Fiz. **31**, 486 (1980) [JETP Lett. **31**, 456 (1980)].

[14]M. Nakahara and K. Maki, Phys. Rev. B **24**, 1045 (1981).

[15]M. J. Rice and E. J. Mele, Phys. Rev. Lett. **49**, 1455 (1982).

[16]B. Horovitz and B. Schaub, Phys. Rev. Lett. **50**, 1942 (1983).

[17]S. A. Brazovskii, N. Kirova, and V. Yakovenko, J. Phys. (Paris) Colloq. **44**, C3-1525 (1983).

[18]J. Tinka-Gammel and J. A. Krumhansl, Phys. Rev. B **27**, 7659 (1983).

[19]J. T. Ho, Phys. Rev. Lett. **48**, 946 (1982).

[20]B. Horovitz, Phys. Rev. Lett. **48**, 1416 (1982).

[21]B. Horovitz, Phys. Rev. B **22**, 1101 (1980).

[22]E. Pytte, Phys. Rev. B **10**, 4637 (1974).

[23]M. J. Rice, A. R. Bishop, and D. K. Campbell, Phys. Rev. Lett. **51**, 2136 (1983).

[24]D. K. Campbell and A. R. Bishop, Phys. Rev. B **24**, 4859 (1981).

[25]R. Jackiw, Rev. Mod. Phys. **49**, 681 (1977).

[26]A. C. Scott, F. Y. F. Chu, and D. W. McLaughlin, Proc. IEEE **61**, 1433 (1973).

[27]A. L. Fetter and M. J. Stephen, Phys. Rev. **168**, 475 (1968).

[28]B. Sutherland, Phys. Rev. A **8**, 2514 (1973).

[29]W. T. Whittaker and G. N. Watson, *A Course in Modern Analysis* (Cambridge University Press, New York, 1943).

[30]K. Maki, Phys. Rev. B **26**, 2181 (1982).

[31]S. Kivelson and B. Horovitz (unpublished).

[32]J. B. Torrance, J. E. Vazquez, J. J. Mayerle, and V. Y. Lee, Phys. Rev. Lett. **46**, 253 (1981).

[33]S. Kagoshima, Y. Kanai, M. Tani, Y. Tokura, and T. Koda, Mol. Cryst. Liq. Cryst. **120**, 9 (1985).

[34]D. K. Campbell, Phys. Rev. Lett. **50**, 865 (1983).

[35]B. Horovitz, J. Phys. C **15**, 175 (1982).

[36]B. Horovitz, Solid State Commun. **41**, 593 (1982).

[37]E. Ehrenfreund, Z. Vardeny, O. Brafman, R. Weagley, and A. J. Epstein, Phys. Rev. Lett. **57**, 2081 (1986).

[38]K. Machida and M. Fujita, Phys. Rev. B **30**, 5284 (1984).

[39]K. Machida, M. A. Lind, and J. L. Stanford, J. Phys. Soc. Jpn. **53**, 4020 (1984).

[40]M. Fujita and K. Machida, J. Phys. Soc. Jpn. **53**. 4395 (1984).

[41]T. W. Hijmans, H. B. Brom and L. J. de Jongh, in Proceedings of the International Conference on Synthetics Metals (Kyoto, 1986), Ref. 3.

[42]J. Tinka Gammel, Phys. Rev. B **33**, 5974 (1986).